



ELSEVIER

Contents lists available at ScienceDirect

## Comptes Rendus Mecanique

www.sciencedirect.com



Thermodiffusion and coupled phenomena / Thermodiffusion et phénomènes couplés

## Soret-driven convection in a porous cavity with perfectly conducting boundaries

Dmitriy Lyubimov<sup>a</sup>, Konstantin Gavrilov<sup>a</sup>, Tatyana Lyubimova<sup>a,b,\*</sup><sup>a</sup> Theoretical Physics Department, Perm State University, Bukireva str. 15, 614990 Perm, Russia<sup>b</sup> Institute of Continuous Media Mechanics UB RAS, Koroleva str. 1, 614013 Perm, Russia

## ARTICLE INFO

## Article history:

Available online 20 April 2011

## Keywords:

Instability  
Filtration convection  
Soret effect

## ABSTRACT

This article deals with two-dimensional Soret-driven convection in a porous cavity with perfectly conducting boundaries heated from below. It is shown that thermodiffusion effect destroys degeneracy existing in the case of single-component fluid. The scenario of the convection onset is discussed. The boundaries of the diffusive state instability to the small-amplitude and finite-amplitude monotonous and oscillatory perturbations are determined.

© 2011 Académie des sciences. Published by Elsevier Masson SAS. All rights reserved.

## 1. Introduction

Convection in a porous medium is widely studied due to the broad field of industrial, geophysical and environmental applications. Different aspects of a filtration convection like double-diffusive convection are discussed in [1]. In [2] the authors carried out numerical and analytical investigation of the Soret-driven convection using Brinkman-extended Darcy model for a sparsely packed porous medium. The flows in a shallow enclosure heated from below are studied for the case of fixed heat flux at the boundaries. The critical Rayleigh number is found to be strongly dependent on the separation factor. Different types of perturbations (monotonic, oscillating and subcritical) exist at different separation factor values.

The present article deals with the onset of two-dimensional Soret-driven convection in a horizontal porous cylinder with perfectly conducting boundaries heated from below. For single-component fluid this problem was studied by Lyubimov [3]. He found out that at supercritical parameter values the problem has infinite number of stationary solutions for arbitrary shape of the cavity. As shown in [4], weak deviation from perfect conditions (finite conductivity of the boundaries, heating non-strictly from below, weak seeping through the boundaries, etc.) may destroy degeneracy, however, the dynamics of the system at supercritical Rayleigh number values reflects the existence of infinite number of stationary solutions in perfect conditions. These results were confirmed experimentally in [5].

The goal of the present work is to study thermodiffusion effect on the onset and dynamical properties of convection in the configuration considered in [3]. In the first part of paper we implement weakly nonlinear analysis to study the dynamical properties of two-dimensional Soret-driven convection in a porous cylinder at small values of the separation factor. In the second part the linear stability of the diffusive state is studied for finite values of the separation factor.

## 2. Problem formulation

We consider the onset of convection in infinite horizontal cylinder of square cross-section filled with the isotropic porous material saturated with the binary fluid (Fig. 1). The upper and lower boundaries of the cylinder are maintained at different

\* Corresponding author at: Institute of Continuous Media Mechanics UB RAS, Koroleva str. 1, 614013 Perm, Russia.

E-mail address: [lyubimova@psu.ru](mailto:lyubimova@psu.ru) (T. Lyubimova).

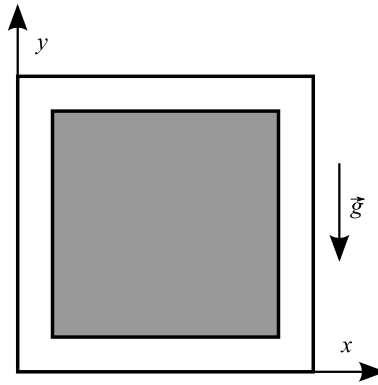


Fig. 1. Problem configuration.

constant temperatures and uniform vertical temperature gradient is imposed on lateral boundaries. All the boundaries are supposed to be rigid and impermeable. The fluid is viscous and incompressible.

It is assumed that the mixture density  $\tilde{\rho}$  linearly depends on temperature deviation from average value  $\tilde{T}$  and solute concentration  $\tilde{C}$ :  $\tilde{\rho} = \tilde{\rho}_0(1 - \beta_1\tilde{T} - \beta_2\tilde{C})$ , where  $\tilde{\rho}_0$  is the average density of the mixture,  $\beta_1$  and  $\beta_2$  are thermal and solutal expansion coefficients, respectively,  $\beta_2 > 0$  if the solute is lighter than the base fluid. The thermodiffusion effect is taken into account, thus the diffusive flux  $\vec{j}$  is proportional to the concentration and temperature gradients  $\vec{j} = -\rho_0 D(\nabla\tilde{C} + \alpha_T\nabla\tilde{T})$ , where  $D$  is the mass diffusivity,  $\alpha_T$  is the thermodiffusion coefficient. These coefficients can be considered as a constant due to the small temperature and concentration variations inside the cavity. Normal thermodiffusion effect corresponds to the case when the light component moves to the warmer area.

Full set of equations describing the filtration Soret-driven convection consists of the Darcy–Boussinesq equation, the continuity equation, the energy equation and the concentration evolution equation [1]:

$$0 = -\frac{1}{\tilde{\rho}_0}\nabla\tilde{p} - \frac{\nu}{K}\vec{\tilde{v}} + g(\beta_1\tilde{T} + \beta_2\tilde{C})\vec{\gamma} \tag{1}$$

$$\text{div}\vec{\tilde{v}} = 0 \tag{2}$$

$$b\frac{\partial\tilde{T}}{\partial t} + \vec{\tilde{v}} \cdot \nabla\tilde{T} = \chi_{\text{eff}}\Delta\tilde{T} \tag{3}$$

$$\tilde{m}\frac{\partial\tilde{C}}{\partial t} + \vec{\tilde{v}} \cdot \nabla\tilde{C} = D(\Delta\tilde{C} + \alpha_T\Delta\tilde{T}) \tag{4}$$

In these equations  $\tilde{p}$  is the pressure,  $\vec{\tilde{v}}$  is the velocity,  $K$  is the permeability,  $\tilde{m}$  is the porosity,  $b$  is the media-fluid heat capacity ratio,  $\chi_{\text{eff}}$  is the effective thermal diffusivity of mixture,  $\vec{\gamma}$  is the vertical unit vector. The slip and impermeability boundary conditions are imposed for the velocity and mass flux ( $\vec{n}$  is the unit vector normal to the boundary):

$$(\nabla\tilde{C} + \alpha_T\nabla\tilde{T}) \cdot \vec{n} = 0, \quad \vec{\tilde{v}} \cdot \vec{n} = 0 \tag{5}$$

The temperatures of the upper and lower boundaries are fixed and constant linear temperature distribution is imposed on the lateral boundaries:

$$\tilde{T}(x=0, L) = \Theta\left(1 - \frac{y}{L}\right), \quad \tilde{T}(y=0) = \Theta, \quad \tilde{T}(y=L) = 0 \tag{6}$$

Eqs. (1)–(4) with the boundary conditions (5), (6) have the solution which corresponds to the diffusive state:

$$\vec{\tilde{v}}_0 = 0, \quad \tilde{T}_0 = \Theta\left(1 - \frac{y}{L}\right), \quad \tilde{C}_0 = \alpha_T\Theta\frac{y}{L} + \text{const} \tag{7}$$

To study the stability of this state we formulate the problem for small perturbations. Choosing appropriate following scales for the length ( $L$ ), time ( $bL^2/\chi_{\text{eff}}$ ), pressure ( $\rho\nu\chi_{\text{eff}}/K$ ), velocity ( $\chi_{\text{eff}}/L$ ), temperature ( $\Theta$ ) and concentration ( $\beta_1\Theta/\beta_2$ ) we rewrite the equations and boundary conditions in the dimensionless form. We restrict ourselves to two-dimensional solutions. In this it is convenient to exclude the pressure and introduce stream function  $\psi$  related to the velocity as  $v_x = \partial\psi/\partial y$ ,  $v_y = -\partial\psi/\partial x$ . To simplify the boundary condition for mass flux we introduce the new variable  $\eta = C - \varepsilon T$ , where  $\varepsilon = -\alpha_T\beta_2/\beta_1$  is the separation factor. Taking into account these assumptions the problem for the dimensionless perturbations is written as follows

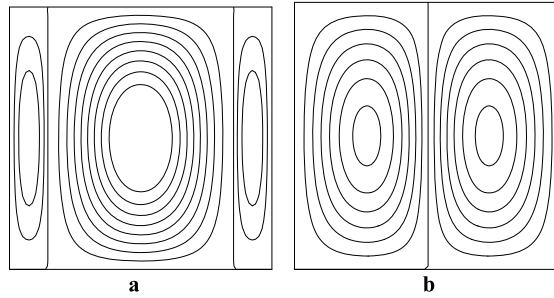


Fig. 2. Stream function for two independent solutions which correspond to the lowest instability level at  $\varepsilon = 0$ .

$$0 = \Delta\psi + R \left( \frac{\partial T}{\partial x} (1 + \varepsilon) + \frac{\partial \eta}{\partial x} \right) \tag{8}$$

$$\frac{\partial T}{\partial t} = \Delta T - \frac{\partial \psi}{\partial x} - J(T, \psi) \tag{9}$$

$$\frac{\partial \eta}{\partial t} = \frac{Le}{m} \Delta \eta - \varepsilon \Delta T - \varepsilon \left( \frac{1}{m} - 1 \right) \left( \frac{\partial \psi}{\partial x} + J(T, \psi) \right) - \frac{1}{m} J(\eta, \psi) \tag{10}$$

$$T|_{\Gamma} = 0, \quad \psi|_{\Gamma} = 0, \quad \frac{\partial \eta}{\partial n} \Big|_{\Gamma} = 0 \tag{11}$$

where  $J$  is the Jakobian and  $\Gamma$  is the boundary of the domain.

The problem (8)–(11) contains the following dimensionless parameters: the Darcy–Rayleigh number  $R = gLK\beta_1\Theta/\nu\chi_{\text{eff}}$ , the separation factor  $\varepsilon = -\alpha_1\beta_2/\beta_1$ , the Lewis number  $Le = D/\chi_{\text{eff}}$  and the normalized porosity  $m = \tilde{m}/b$ .

### 3. Amplitude equations for small supercriticalities

As it was shown in [3], in the case of single-component fluid the problem has infinite number of stationary solutions for arbitrary shape of the cavity when Rayleigh number exceeds some critical value. Indeed, in this case the linear problem for critical monotonous perturbations has the form:

$$\Delta\psi_1 + R \frac{\partial T_1}{\partial x} = 0, \quad \Delta T_1 - \frac{\partial \psi_1}{\partial x} = 0, \quad T_1|_{\Gamma} = \psi_1|_{\Gamma} = 0 \tag{12}$$

This problem has a remarkable property – it is invariant with respect to the change of variables  $(\psi_1 \rightarrow \sqrt{R}T_1, T_1 \rightarrow -\psi_1/\sqrt{R})$  [3]. The general solution of (12) is represented as the superposition of two independent particular solutions  $\varphi$  and  $\vartheta$ :

$$\psi_1 = \sqrt{R}(\alpha\varphi + \beta\vartheta), \quad T_1 = \alpha\vartheta - \beta\varphi \tag{13}$$

In the case of square cavity, it is possible to specify the spatial distribution of  $\varphi$  and  $\vartheta$  and the spectra of critical Rayleigh numbers  $R^*$ :

$$\varphi_{nk} = \sin \pi kx \cos \pi \sqrt{n^2 + k^2} \left( x - \frac{1}{2} \right) \sin \pi ny, \quad \vartheta_{nk} = \sin \pi kx \sin \pi \sqrt{n^2 + k^2} \left( x - \frac{1}{2} \right) \sin \pi ny \tag{14}$$

$$R_{nk}^* = 4\pi^2(n^2 + k^2), \quad n, k \in \mathbb{N} \tag{15}$$

Stream function fields for two independent solutions which correspond to the lowest instability level, are shown in Figs. 2a and 2b. Temperature field for the first of these solutions looks like stream function field for the second solution (Fig. 2b) and temperature field for the second solution – like stream function field for the first solution (Fig. 2a).

As shown in [3], in the case of single-component fluid the nontrivial supercritical solutions of nonlinear problem organize one-parametric family. Weak deviations from perfect conditions (finite conductivity of the boundaries, heating non-strictly from below, weak seeping through the boundaries) may destroy degeneracy [4].

Let us apply the same technique as in [4] to study the behavior of the nonlinear system (8)–(11) at small supercriticalities. We expand stream function, temperature, concentration, separation factor, Rayleigh number in the series of formal small parameter. Using the multiple-scale method and assuming that the separation factor  $\varepsilon$  is small enough we could apply a standard method to obtain a dynamical system for amplitudes  $\alpha$  and  $\beta$ . In accordance with this technique a sequence of heterogeneous systems for each order of formal small parameter is derived. The conditions for the solution existence allow one to construct the dynamical system:

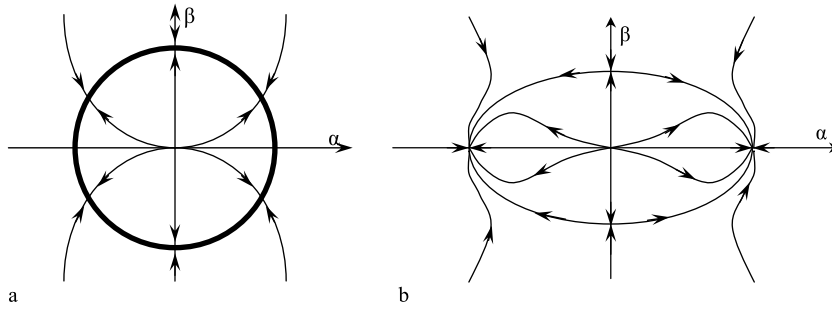


Fig. 3. Typical phase portraits for the dynamical system in the absence of thermodiffusion effect (a) and in the presence of thermodiffusion effect (b).

$$\begin{aligned}
 d_1 \frac{d\alpha}{dt} &= \alpha [(d_3 + d_5 Le^{-1})\varepsilon R^* + d_3(R - R^*) - (\alpha^2 + \beta^2)d_4 R^*] \\
 d_2 \frac{d\beta}{dt} &= \beta [(d_3 + d_6 Le^{-1})\varepsilon R^* + d_3(R - R^*) - (\alpha^2 + \beta^2)d_4 R^*]
 \end{aligned}
 \tag{16}$$

where the coefficients  $d_1 = 0.0979$ ,  $d_2 = 0.1521$ ,  $d_3 = 0.5554$ ,  $d_4 = 0.2313$ ,  $d_5 = 1.1646$  and  $d_6 = 0.7851$  are calculated using the standard procedure. Fig. 3 demonstrates the comparison of typical phase portraits in the absence and in the presence of thermodiffusion effect. As shown in [3], in the absence of thermodiffusion the stationary solutions are located on the circle (bold line in Fig. 3a) and all of them are stable. At any non-zero values of  $\varepsilon$  degeneracy is destroyed. In this case, when Rayleigh number exceeds a threshold value ( $R > R^*$ ), instead of infinite number of stationary solution, we have one trivial and four nontrivial solutions (Fig. 3b). The linear analysis of stationary solutions of the system (16) shows that two of these solutions with amplitudes  $\hat{\alpha}$  and  $\hat{\beta}$  are stable:

$$\hat{\alpha}_{1,2} = \pm \sqrt{((d_3 + d_5 Le^{-1})\varepsilon R^* + d_3(R - R^*)) / d_4 R^*}, \quad \hat{\beta} = 0
 \tag{17}$$

One of solutions (17) corresponds to one-vortex flow in the clockwise direction and the other – to the counter-clockwise flow. As the result, for small values of the separation factor the nonlinear system (8)–(10) has even spatial pattern.

The degeneracy destruction scenario is similar to the one observed in [4] for finite thermal conductivities of the boundaries.

#### 4. Numerical method

To carry out investigation of the convection onset at finite values of the separation factor  $\varepsilon$  the following numerical method was applied. The finite-difference technique was used to solve Eqs. (8)–(10) with the boundary conditions (11). The central difference scheme was used for the discretization of spatial derivatives and backward Euler method – for the discretization of time-derivatives. The alternating direction implicit method was applied to solve the discrete linear algebraic systems derived from the energy and concentration equations. The Darcy equation was solved with the help of successive over-relaxation method. The uniform mesh with number of nodes equal to  $50 \times 50$  was employed.

In accordance with linear stability analysis, the solution of linear problem (8)–(11) looks like

$$\psi(t, x, y) = \bar{\psi}(x, y)e^{\lambda t}, \quad T(t, x, y) = \bar{T}(x, y)e^{\lambda t}, \quad \eta(t, x, y) = \bar{\eta}(x, y)e^{\lambda t}
 \tag{18}$$

To compute the maximum increment in spectra we apply the following technique based on *Arnoldi method* [6]. The evolution problem for the perturbations (8)–(11) is written as

$$\frac{df}{dt} = \mathfrak{S}f
 \tag{19}$$

where  $f$  is the vector which components equal to the stream function, temperature and  $\eta$  at computational grid nodes  $f = (\psi, T, \eta)$ ,  $\mathfrak{S}$  is linear operator of the linear problem (8)–(11). If  $f_1$  is chosen as an initial basis vector then the other  $N$  vectors are constructed by the rule

$$f_{i+1} = \mathfrak{S}f_i, \quad 1 < i \leq N
 \tag{20}$$

We can define the scalar product operation  $\langle f_i f_j \rangle$  for the vectors  $f_i$  and  $f_j$  as the sum over all grid nodes of stream function, temperature and chemical potential values' products. The spectra of increments is the set of eigenvalues for the problem

$$AY = \lambda BY, \quad A_{ij} = \langle f_i \mathfrak{S} f_j \rangle, \quad B_{ij} = \langle f_i f_j \rangle
 \tag{21}$$

where  $Y$  is a vector with dimension  $N$ , in the present paper we choose  $N = 3$  for computations.

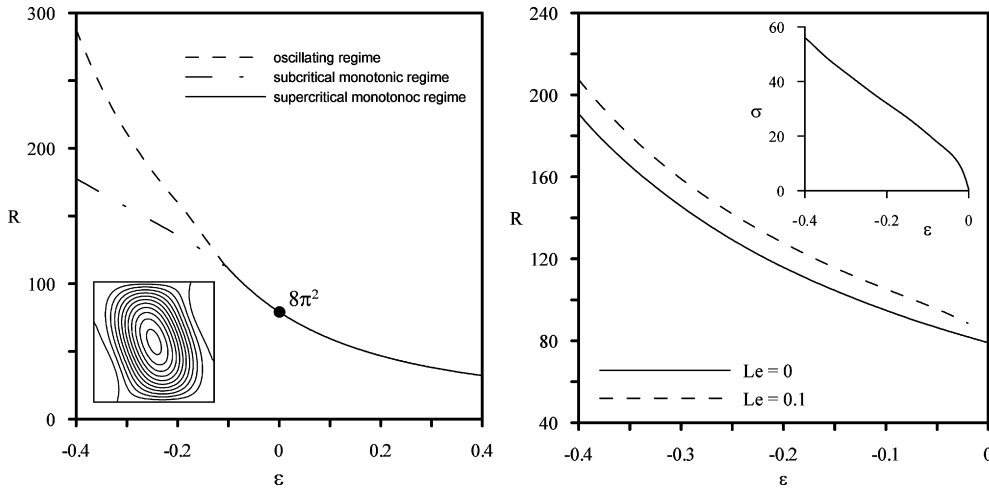


**Fig. 4.** Stability map ( $m = 0.75$ ). (a)  $Le = 1$ , solid line corresponds to the monotonic supercritical threshold, dashed line corresponds to the oscillatory threshold, dash-dot line corresponds to the monotonic subcritical threshold. (b) The oscillatory thresholds for different Lewis numbers, solid line corresponds to  $Le = 0$  and dashed line corresponds to  $Le = 0.1$ . Additional fragment in the upper right corner illustrates the frequency variation with the separation factor.

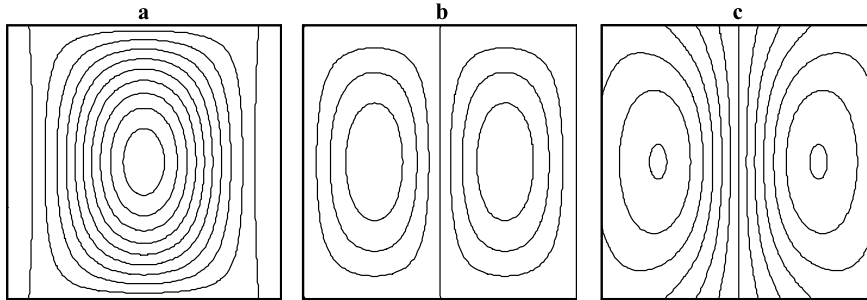


**Fig. 5.** Stream function (a), temperature (b) and concentration (c) distributions ( $m = 0.75, Le = 1, \epsilon = 0.1, R = 59$ ).

**5. Numerical results**

In Fig. 4a the stability map in the parameter plane *separation factor*–*Rayleigh number* is presented for  $Le = 1$ . In accordance with (15), for  $\epsilon = 0$ , the critical Rayleigh number is equal to  $8\pi^2$ , this point is marked with a full circle at the graph center. For normal thermodiffusion effect ( $\epsilon > 0$ ) the stationary flow arises at Rayleigh number higher than the critical one (solid line in Fig. 4a).

The spatial structures of stream function, temperature and concentration obtained for  $m = 0.75, Le = 1, \epsilon = 0.1, R = 59$  are presented in Fig. 5. We investigate one-vortex flow which carries warm fluid from one half of the cavity to the other. The stream function pattern is similar to the one presented in Fig. 2a and the temperature pattern is similar to Fig. 2b. This result is in agreement with the results of weakly nonlinear analysis discussed in Section 3.

In Fig. 4a three types of stability boundaries are plotted: the solid line corresponds to the monotonic supercritical threshold, the dashed line corresponds to the oscillatory threshold, the dash-dot line corresponds to the monotonic subcritical threshold. As one can see, in case of normal thermodiffusion, the separation factor growth leads to the lowering of critical Rayleigh number. When anomalous thermodiffusion is enhancing, the diffusive state is stabilized ( $\epsilon < 0$ ). If the separation factor exceeds some value ( $\epsilon^* = -0.14$ ) the oscillatory instability develops. The critical Rayleigh number is growing (dashed line in Fig. 4a) with the amplification of anomalous thermodiffusion.

The  $\epsilon^*$ -point position where the oscillatory instability appears depends on the Lewis number. When the Lewis number is small ( $Le \ll 1$ ) and thermal conduction mechanism is much stronger than the diffusion mechanism, the oscillatory perturbations born at small anomalous thermodiffusion values ( $|\epsilon^*| \ll 1$ ). The oscillatory thresholds for different Lewis numbers are shown in Fig. 4b: solid line corresponds to  $Le = 0$  and dashed line corresponds to  $Le = 0.1$ . Additional fragment in the upper right corner illustrates the frequency variation with the separation factor. When the diffusion–thermal conductivity ratio is growing the  $\epsilon^*$ -point position moves to the domain with higher values of Rayleigh number.  $Le = 1$  is typical value of Lewis number for liquid mixture and  $Le = 0.01$  – for gaseous mixture. Lewis number decreasing destabilizes the diffusive state for normal and anomalous thermodiffusion.

## 6. Conclusion

The conditions for the onset of filtration convection in 2D cavity of square cross-section filled with porous material and binary mixture are studied. It is found that any weak thermodiffusion effect destroys the degeneracy existing in the case of single-component fluid. For small values of the separation factor the spatial pattern with even temperature distribution arises in the system. For finite values of the separation factor the linear stability of the diffusive state is studied numerically by finite-difference method. The instability thresholds are calculated for monotonic and oscillatory perturbations.

## References

- [1] D.A. Nield, A. Bejan, *Convection in Porous Media*, Springer Science, Business Media, Inc, New York, 2006.
- [2] M. Bourich, M. Hasnaoui, A. Amahmid, M. Mamou, Onset of convection and finite amplitude flow due to Soret effect within a horizontal sparsely pecked porous enclosure heated from below, *Int. J. Heat and Fluid Flow* 26 (2005) 513–525.
- [3] D.V. Lyubimov, On the convective flows in the porous medium heated from below, *J. Appl. Mech. Tech. Phys.* 16 (1975) 131–137 (in Russian).
- [4] D.V. Lyubimov, *Dynamic Properties of Thermal Convection in Porous Medium: Instabilities in Multiphase Flows*, Plenum Publishing Co., London, 1993.
- [5] A.F. Glukhov, D.V. Lyubimov, G.F. Putin, Convective motions in a porous medium near the equilibrium instability threshold, *Sov. Phys. Dokl.* 23 (1978) 22–24.
- [6] Y. Saad, *Numerical Methods for Large Eigenvalue Problems*, Manchester University Press, Manchester, 1992.